9-2009

Bit Error Rates for Ultrafast APD Based Optical Receivers: Exact and Large Deviation Based Asymptotic Approaches

Peng Sun
University of New Mexico

Majeed M. Hayat
Marquette University, majeed.hayat@marquette.edu

Abhik K. Das
Indian Institute of Technology

Bit Error Rates for Ultrafast APD Based Optical Receivers: Exact and Large Deviation Based Asymptotic Approaches

Peng Sun
University of New Mexico, Albuquerque, NM
Majeed M. Hayat
University of New Mexico, Albuquerque, NM
Abhik K. Das
Indian Institute of Technology, Kanpur, India

Abstract:
Exact analysis as well as asymptotic analysis, based on large-deviation theory (LDT), are developed to compute the bit-error rate (BER) for ultrafast avalanche-photodiode (APD) based optical receivers assuming on-off keying and direct detection. The effects of intersymbol interference (ISI), resulting from the APD's stochastic avalanche buildup time, as well as the APD's dead space are both included in the analysis. ISI becomes a limiting factor as the transmission rate approaches the detector's bandwidth, in which case the bit duration becomes comparable to APD's avalanche buildup time. Further, the effect of dead space becomes significant in high-speed APDs that

employ thin avalanche multiplication regions. While the exact BER analysis at the generality considered here has not been reported heretofore, the asymptotic analysis is a major generalization of that developed by Letaief and Sadowsky [IEEE Trans. Inform. Theory, vol. 38, 1992], in which the LDT was used to estimate the BER assuming APDs with an instantaneous response (negligible avalanche buildup time) and no dead space. These results are compared with those obtained using the common Gaussian approximation approach showing the inadequacy of the Guassian approximation when ISI noise has strong presence.

Keywords

SECTION I. Introduction

Inp-Based avalanche photodiodes (APDs) are arguably the photodetectors of choice in today's ultrafast long-haul and metro-area lightwave systems. The popularity of APDs in high-speed receivers is attributed to their ability to provide high internal optoelectronic gain, which allows the photo-generated electrical signal to dominate the thermal (or Johnson) noise in the pre-amplifier stage of the receiver module without the need for optical pre-amplification of the received optical signal [1]. The optoelectronic gain results from the cascade, or avalanche, of electron and hole impact ionizations that take place in the high-field intrinsic multiplication layer of the APD [2]. Due to its stochastic nature, however, this avalanche multiplication process is inherently noisy, resulting in random fluctuations in the gain. Thus, the benefit of the gain is accompanied by a penalty: the shot noise present in the photo-generated electrical signal is accentuated according to the APD's excess noise factor, which is a measure of uncertainty associated with the stochastic nature of the APD's gain [2]. In addition, the APD's avalanche buildup time, which is the time required for the cascade of impact ionizations to complete, also limits the receiver performance by inducing intersymbol interference (ISI) at high bit rates.

Thanks to remarkable advances in APD design and fabrication in recent years, some of these challenges have been addressed through the use of APDs with separate absorption and multiplication layers (often referred to as SAM APDs) [3], APDs with thin multiplication regions [4]–[5][6][7][8][9], impactionization engineering of the multiplication region [10], [11], as well as employing clever light-coupling strategies such as edge and evanescent coupling [12]. In particular, APDs with thin multiplication regions have been shown to have reduced buildup time and reduced gain fluctuations [2], [6], [9], [13], [14], making them suitable for 10 Gbps transmission rate.

Clearly, the ability to understand and predict the performance of APD-based receivers at high speeds, for which the ISI and Johnson noise are pressing problems, relies upon the presence of an accurate probabilistic model of the APD that characterizes the evolution of the avalanche multiplication process. The traditional McIntyre theory for the APD's gain statistics [15] has been shown to be inadequate for APDs with thin multiplication regions because of the dead space [4]–[5][6][7][8], which is the minimum distance that a newly generated carrier must travel before becoming capable of impact ionizing. The dead space is very significant in thin multiplication regions and it is neglected by the McIntyre theory. Subsequently, a great many works were reported that dealt specifically with novel analytical probabilistic models for avalanche multiplication that can properly capture the dead-space effect [16]–[17][18][19]. For its completeness and generality, in this paper we will employ the probabilistic model recently developed by Sun et al. [19], which enables us to compute the probability generating function associated with the joint probability distribution function (PDF) of the gain and the avalanche-buildup time. In addition, a parametric model, using the gain and the buildup time as parameters, was also developed in [19] to approximate the APD's stochastic impulse-response function, thereby allowing us for the first time here to compute the moment-generating function (MGF) of the APD's stochastic impulse

response. This further enables us to compute the MGF of the output of the APD-based integrate-and-dump receiver for the first time to the best of our knowledge.

Exact calculation of the bit-error rate (BER) in the absence of ISI effects (namely, when the impulse-response function of the APD is assumed to be a delta function, or equivalently, when the avalanche multiplication process is assumed to be instantaneous) has been considered by Personik [20] for APDs with no dead space, and subsequently by Hayat et al. with the inclusion of the dead-space effect [21]. There are also a number of approximate methods for calculating the receiver BER in the absence of ISI that have been developed over the years; these include the Gaussian approximation [22], Chernoff bounds [22], and the saddle-point approximation [23]. One of the most elegant methods, and one that is most relevant to this paper, is the work by Letaief and Sadowsky [24] in which a probabilistic asymptotic analysis method, based on large-deviations theory (LDT), was developed yielding an excellent approximation of the BER. Their technique yields a probabilistic equivalent to the accurate saddle-point approximation [23]. In an earlier paper, Sadowsky and Bucklew also proposed an efficient Monte-Carlo simulation method, also based on LDT, that facilitates the efficient estimation of the BER [25]. However, the MGF of APD's gain used in their analysis comes from McIntyre's model [15], which is applicable only to low-speed APDs with thick multiplication regions in which the dead-space effect can be ignored. Recently, Choi and Hayat [26] modified the method reported in [24], [25] to include the dead-space effect. Nonetheless, all these works assume the APD is instantaneous.

The literature on BER calculation for APD-based receivers with the inclusion of ISI is fairly sparse. This is primarily due to the complexity in characterizing the statistics of the stochastic impulse-response function of APDs. The works reported in [19], [21], for example, include an analysis of BER for non-instantaneous APDs with the inclusion of the dead space using a Gaussian approximation for the PDF of the receiver output, albeit with the exact first-order and second-order statistics of the impulse response. Motivated by the rapid increase in bandwidth demand and by high-speed photoreceivers, Groves and David [27] have recently performed a Monte-Carlo analysis of integrate-and-dump receivers including the effects of carrier velocity, the dead space, and the width of the APD's multiplication region. In particular, they have estimated the PDFs of the output of APD-based integrate-and-dump receivers and shown that their shapes are not Gaussian in general. To the best of our knowledge, no exact nor approximate analytical theory has been reported heretofore for the calculation of the BER that address both the dead-space effect and ISI. In this paper, we provide an exact analytical method for calculating the BER as well as an asymptotic approximation based upon LDT. To this end, we adopt the exact model for the joint probability distribution function for the gain and the buildup time as well as the parametric model for the impulse-response function available from our earlier work [19]; the receiver's BER is then calculated exactly. We also exploit our knowledge of the MGF of the APD's impulse response function to extend the LDT-based asymptotic analysis developed by Letaief and Sadowsky [24] to include the effects of ISI and dead space. Finally, we investigate the behavior of BER in ultra-fast transmission regime (up to 60 Gbps) where both ISI and the dead space are significant and compared the exact and asymptotic results to those obtained using a Gaussian approximation.

The remainder of this paper is organized as follows. In Section II we describe the general mathematical model for APD-based integrate-and-dump receiver. In Sections III and IV, we develop the theory for computing the exact and asymptotic BERs, respectively, and the numerical results are presented in Section V. Finally, Section VIdraws the conclusions.

SECTION II. Receiver Model and Moment Generating Function

A. Preliminaries

A typical on-off keying (OOK) optical communication system employing an APD-based intergrate-and-dump receiver is schematically shown in Fig. 1. Consider a received optical pulse, representing an information bit "1," in the time interval $[0, T_b]$, where T_b represents the duration of each bit. We will refer to this time interval as the "current" bit. The energy of the optical pulse can be thought of as a stream of photons; the arrival times of photons obey a Poisson process whose mean rate is proportional to the instantaneous optical power in the pulse [2]. When any of these photons is absorbed by the APD (with a probability equal to the APD's quantum efficiency), it generates what is called a *primary electron-hole pair*, which starts an avalanche process yielding a realization of the stochastic impulse-response function of the APD. The aggregate of all such the realizations of the impulse-response function, one for each absorbed photon, yields the photocurrent corresponding the optical pulse in question.

Fig. 1: A schematic diagram of an OOK optical communication system employing an APD-based integrate and dump receiver.

Let G_i and T_i denote the gain and duration of the impulse-response function resulting from the ith photon, and let $\tau_i \in [0, T_b]$ represent the instant of absorption of the ith photon. According to our earlier work [19], the impulse-response function induced by this photon absorbtion, denoted by $I(t; \tau_i)$, can be modeled by a rectangular function whose duration and area are random. More precisely,

$$I(t; \tau_i) = (G_i/T_i)\mathbf{1}_{[\tau_i, \tau_i + T_i)}(t), \text{ (1)}$$

where $1_{[a,b)}(t) = 1$ for $a \leq t < b$ and 0 otherwise. If we conveniently define $I_i(t - \tau_i) \triangleq \mathbf{1}_{[\tau_i, \tau_i + T_i)}(t)$, then by summing up the contributions from all photons in the interval $[0, T_b]$ we obtain the photocurrent generated by the received optical pulse in the interval $[0, T_b]$,

$$\chi_0(t) = \sum_{i:0 \leq \tau_i < T_b} \frac{G_i}{T_i} I_i(t - \tau_i). \text{ (2)}$$

Similarly, the photocurrent generated by the kth *earlier* optical pulse, namely by the photons absorbed in the time interval $[-kT_b, (-k+1)T_b], k \geq 1$, can be written as

$$\chi_k(t) = \sum_{i:-kT_b \leq \tau_i < (-k+1)T_b} \frac{G_i}{T_i} I_i(t - \tau_i). \text{ (3)}$$

Now let b_k denote an independent and equiprobable $\{0,1\}$-valued random sequence representing the binary information in the kth bit; namely, $b_k = 1$ if there is a optical pulse between $[-kT_b, (-k+1)T_b]$ and $b_k = 0$ otherwise. Hence, the total photocurrent at time $t \in [0, T_b]$ resulting from all photons can be compactly written as $\sum_{k=0}^{\infty} b_k \chi_k(t)$. Note that this gives a decomposition of the total photocurrent in terms of photocurrent contributions, χk(t), by photons from distinct bits. A very useful consequence of this decomposition is that these contributions are statistically independent; this will greatly simplify the analysis leading to the MGF of the receiver output developed in the following section. Note that we have implicitly assumed that the APD yields zero current when the information bit is "0." In actuality, however, both stray photons and dark current, the latter being the current generated by the thermally generated electron and hole

pairs in the APD, do generate a current. Nonetheless, the above model can be adapted to accommodate dark current by including stray-photon and thermal-generation rates. In this paper, however, we will not consider dark current as the focus is on the BER formulation; these effects are considered elsewhere [27].

The output of the integrate-and-dump receiver corresponding to the current bit (index $k = 0$) comprises the integral of the photocurrent over the interval $[0, T_b]$. More precisely, the receiver's output is

$$y_\lambda = \int_0^{T_b} \sum_{k=0}^{\infty} b_k \chi_k(t) dt \text{ , (4)}$$

where the subscript λ refers to the average number of photons per optical pulse. If we define

$$r_k = \int_0^{T_b} \chi_k(t) dt, k = 0,1,2, \dots \text{ (5)}$$

then we have

$$y_\lambda = \sum_{k=0}^{\infty} b_k r_k \text{ . (6)}$$

Note that only the term r_0 conveys information from the optical pulse in the current bit; on the other hand, the components $r_k, k \geq 1$, are merely ISI terms arising from earlier bits. Moreover, since the terms of the sequence χ_k are mutually independent, the terms of the sequence r_k are also mutually independent. By substituting (3) into (5), we obtain

$$r_k = \sum_{i:-kT_b \leq \tau_i < (-k+1)T_b} \int_0^{T_b} \frac{G_i}{T_i} I_i(t - \tau_i) dt \text{ . (7)}$$

Now observe that the quantity defined as

$$a_k(\tau_i) \triangleq \int_0^{T_b} \frac{G_i}{T_i} I_i(t - \tau_i) dt \text{ (8)}$$

is the receiver output in response to a photon absorbed by the APD at time τ_i in the kth previous bit interval. With this definition, the receiver output in response to the kth previous bit, assuming a one bit, can be rewritten alternatively as

$$r_k = \sum_{i:-kT_b \leq \tau_i < (-k+1)T_b} a_k(\tau_i) \text{ . (9)}$$

For the decision rule, we will consider a threshold rule with a decision threshold γ_λ. In this paper, we follow [24] in undertaking a simple approximation of the optimal threshold as

$$\gamma_\lambda \triangleq \gamma \lambda, \text{ (10)}$$

and further define

$$\gamma = \frac{1}{2\lambda} (E[y_\lambda|b_0 = 1] + E[y_\lambda|b_0 = 0]), \text{ (11)}$$

where as before λ is the average number of photons per bit, namely, $\lambda \triangleq T_b/E[\tau_{i+1} - \tau_i]$. Note that γ is a normalized threshold (by λ); the normalization is done to remove the dependency of γ on λ. By using (6), we obtain $\gamma = \frac{1}{2\lambda} \sum_{k=0}^{\infty} E[r_k]$, which can be further simplified, using (5) and (3), to yield

$$\gamma = E[G]/2. \text{ (12)}$$

Note that γ is half of the average gain of the APD. The BER is then defined as

$$P_b = \frac{1}{2}\left(P\{y_\lambda \le \gamma\lambda | b_0 = 1\} + P\{y_\lambda > \gamma\lambda | b_0 = 0\}\right). \text{ (13)}$$

B. Moment generating function of the receiver output

In the previous section, we have expressed the photocurrent generated by the kth earlier optical pulse in terms of realizations of the stochastic impulse-response functions that correspond to individual photons (see (3)). We now use (3) and (5) to derive the MGF of r_k. We begin by dividing the kth previous bit interval, $[-kT_b, (-k + 1)T_b]$, into N equal time-slots. Observe that the photocurrent generated by the kth earlier optical pulse can now be recast as

$$\chi_k(t) = \sum_{i=1}^{N} \sum_{j=0}^{n_i} \frac{G_{ij}}{T_{ij}} I_{ij}(t - \tau_{ij}),$$

where n_i is the random number of photon absorptions in the ith time slot, which is a Poisson random variable with mean value of λ/N; the quantity τ_{ij} is the instant of the jth absorption in the ith time slot, $(i - 1)T_b/N \le \tau_{ij} < iT_b/N$. By recalling the definition of $a_k(\tau_{ij})$ (8), the quantity r_k can be recast as

$$r_k = \sum_{i=1}^{N} \sum_{j=0}^{n_i} a_k(\tau_{ij}). \text{ (14)}$$

The conditional MGF of $a_k(\tau_{ij})$ given $\tau_{ij} = \xi$, denoted by $A_k(\mu|\xi)$, is given by

$$A_k(\mu|\xi) = E[\exp(\mu a_k(\tau_{ij}))|\tau_{ij} = \xi] \text{ (15)}$$

and it can be calculated by averaging $\exp \mu a_k(\tau_{ij}))$ over all possible pairs of G_{ij} and T_{ij} with respect to the joint PDF of G_{ij} and T_{ij}. Note that $a_k(\tau_{ij})$ is independent of $a_k(\tau_{ih})$ for $j \ne h$, and so is $a_k(\tau_{ij})$ of $a_l(\tau_{ij})$, for $k \ne l$. By taking the limit as $N \to \infty$ in each r_k and averaging over the Poisson number of photons process (represented by the arrival times $\tau'_{ij}s$) in each slot, we obtain the MGF of r_k, denoted by $R_k(\mu)$. More precisely,

$$R_k(\mu) = \exp\left(\lambda\left[\frac{1}{T_b}\int_0^{T_b} A_k(\mu|\xi)d\xi - 1\right]\right). \text{ (16)}$$

Additionally, we refer to the logarithm of the conditional MGF of $y\lambda$ given b_0, normalized by λ, as $\phi_\lambda(\mu|b_0)$. More precisely,

$$\phi_\lambda(\mu|b_0) \triangleq \frac{1}{\lambda}\log(E[\exp(\mu y_\lambda)|b_0]). \text{ (17)}$$

Using (6) and considering the fact that r_k's are independent of each other, it is derived that

$$\phi_\lambda(\mu|b_0) = \begin{cases} \frac{1}{\lambda}\log\left[R_0(\mu)\prod_{k=1}^{\infty}(\frac{1}{2}+\frac{1}{2}R_k(\mu))\right], \\ \qquad\text{for } b_0 = 1, \text{(18a)} \\ \frac{1}{\lambda}\log\left[\prod_{k=1}^{\infty}(\frac{1}{2}+\frac{1}{2}R_k(\mu))\right], \\ \qquad\text{for } b_0 = 0. \text{(18b)} \end{cases} \qquad \text{(18b)}$$

In Sec. IV, the limit of $\phi_\lambda(\mu|b_0)$ as $\lambda \to \infty$ will be derived, enabling us apply large-deviation theory to estimate the BER. But first, we pursue the exact numerical calculation of the BER.

SECTION III. Exact Analysis

The exact approach undertaken for calculating the BER is based on numerically inverting the MGF of the receiver output. Note that the Fourier transform, $X(f)$, of a probability density function (pdf), $x(t)$, is its moment generating function $M_x(\mu)$ evaluated at $\mu = -i2\pi f$. Therefore, given the MGFs of the components r_k's, the exact pdfs of r_k's can be calculated by an inverse Fourier transform. When implementing this inversion numerically, the discrete fourier transform (DFT) is adopted; thus, the conversion from pdf to a probability mass function (pmf) is necessary. (We have tested our code on a Gaussian MGF, corresponding to a Gaussian random variable with a mean of 5000 and a standard deviation of 500, and achieved an absolute error of 10^{-15} in estimating the Gaussian pdf uniformly in the range [0, 10000].)

In our calculations we selected an InP-based APD with a 100 nm multiplication layer. An electrical field of 8.836×10^5 V/cm was assumed in the multiplication layer of the APD, corresponding to an average gain of 10.65 and a 3-dB bandwith of 20 GHz. For this width of the multiplication region, the dead space is substantial and must be accounted for [4]. The joint pdf of the gain and buildup time was numerically calculated using the renewal theory reported in [19], which incorporates the dead-space effect. It is known that the avalanche duration, T, is finite almost surely as long as the electric field is below the avalanche breakdown condition (as in our case). Therefore, we can justify setting an upper limit, say m, in the summation in (6) to yield a simplifying approximation of the receiver output $y\lambda$. More precisely, we have the approximation $y_\lambda = \sum_{k=0}^{m} b_k r_k$; an appropriate value of m can be determined by trial and error.

With the choice of the aforementioned APD, we have computed the MGFs $A_k(\mu|\xi)$ and $R_k(\mu)$ according to (15) and (16), respectively, and the pdfs of r_0, r_1 and r_2, denoted by $f_{r,0}(x), f_{r,1}(x)$ and $f_{r,2}(x)$, respectively, were calculated from their MGFs. Figure 2 illustrates the pdfs of the components r_0, r_1 and r_2. (In our numerical calculations, we have approximated r_k to its closest integer values, which also corresponds, physically, to the number of electron and hole pairs.) It is observed that $P\{r_1 = 0\} = 0.50$ and $P\{r_2 = 0\} = 0.53$, which are represented by the point-mass functions at zero; this justifies our selection of $m = 2$. In addition, the pdfs of $f_{r,0}$ and $f_{r,1}$ exhibit a clear asymmetric shape as the right tail decays slower than the left tail.
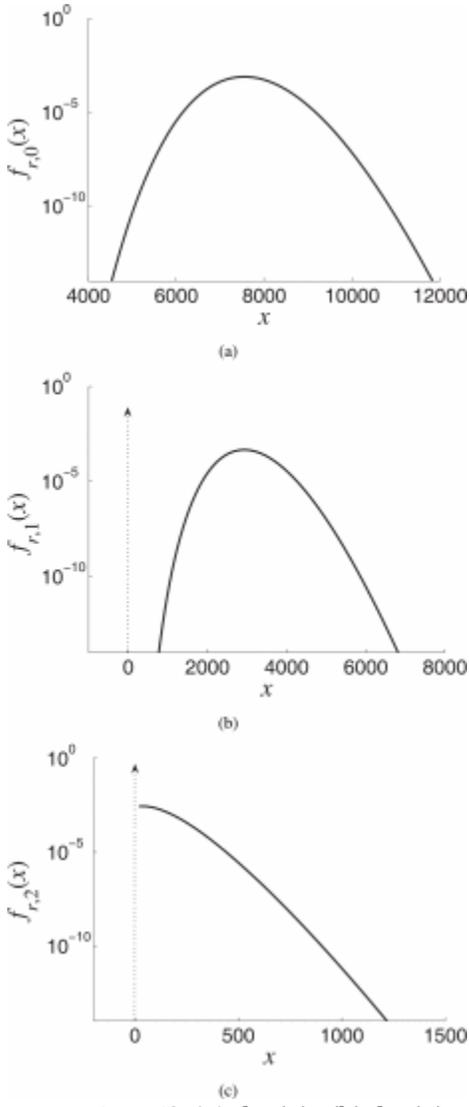
Fig. 2: The pdfs (a) $f_{r,0}(x)$; (b) $f_{r,1}(x)$; and (c) $f_{r,2}(x)$. The bit rate is 40 Gbps and 1000 photons per bit are assumed on average.

Since b_i takes value of 0 or 1 with equal probability, then the pdf of the product $b_i r_i$, denoted by $f_{br,i}$ can be calculated as

$$f_{br,i}(x) = \frac{1}{2}\delta(x) + \frac{1}{2}f_{r,i}(x). \text{ (19)}$$

Hence, by the independency between r_0, r_1 and r_2, the pdf of Y_λ conditional on b_0, denoted by $f_y(x|b_0)$, can be obtained by the convolutions

$$f_y(x|b_0 = 0) = f_{br,1}(x) * f_{br,2}(x),$$

and

$$f_y(x|b_0 = 1) = f_{br,0}(x) * f_{br,1}(x) * f_{br,2}(x).$$

Figure 3 shows the pdf $f_y(x|b_0)$ for the cases of $b_0 = 0$ and $b_0 = 1$. Note that the receiver's output, $y\lambda$, exhibits a bi-modal distribution corresponding to the two possible states of the current bit. The BER can now be calculated according to (13). The results are shown in Section V.
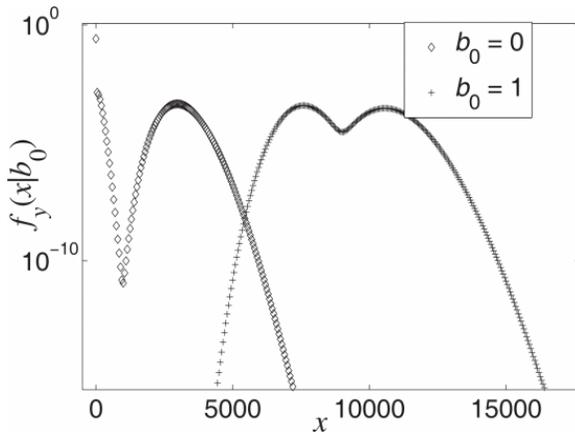
Fig. 3: The pdfs of $y\lambda$ conditional on the current bits is "0" and "1." The bit rate is 40 Gbps and 1000 photons per bit are assumed on average.

We next obtain an asymptotic estimate of the BER as $\lambda \to \infty$.

SECTION IV. Large Deviation Theory

For the undertaken single threshold detection problem, an error occurs when either the receiver's output $y\lambda$ is below $\gamma\lambda$ given $b_0 = 1$, or above $\gamma\lambda$ given $b_0 = 0$. The detection errors become rare events as the intensity of the optical stream increases; more precisely, $P\{y_\lambda \geq \gamma_\lambda | b_0 = 0\} \to 0$ and $P\{y_\lambda < \gamma_\lambda | b_0 = 1\} \to 0$ as $\lambda \to \infty$. To effectively evaluate the asymptotic performance of the receiver's BER, we resort to LDT.

Generally speaking, LDT deals with the probability of rare events and its rate of convergence to zero in an appropriate asymptotic setting. While LDT had already been applied to detection in optical communications, to the best of our knowledge, it has not been applied to the setting of this paper, where ISI is considered. Letaief and Sadowsky [24] employed Cramér's theorem [28] to estimate the BER for direct detection APD-based integrate-and-dump receiver. In their work, they assumed that the detector response to photons is instantaneous, in which case ISI becomes absent and the contributions of distinct photons to the receiver output are independent and identically distributed. More recently, Hayat and Choi [26] modified Letaief and Sadowsky's method to include the dead-space effect by introducing new MGF for the APD's gain that takes into account the dead-space effect. Nonetheless, the assumption of instantaneous-detector assumption was maintained in [26]. In this paper and as a result of ISI, the contributions of photons to the receiver output are not identically distributed, albeit they are independent. To address this problem, we will utilize our probabilistic characterization of the receiver output (described in Section II) in conjunction with the theorem of Gärtner and Ellis [28], [29]. The latter is a generalization of Cramér's theorem [28], which is for i.i.d. random sequences, to arbitrary random sequences. We begin our analysis by briefly reviewing the theorem of Gärtner and Ellis [28].

IV. Theorem 1 (Gärtner and Ellis [28])

Let $\{Y_n\}$ be a sequence of random variables and define $\phi_n(\mu) \triangleq \frac{1}{n}\log E[\exp(\mu Y_n)]$. Assume further that $\phi(\mu) \triangleq \lim_{n\to\infty} \phi_n(\mu)$ exists for all $\mu \in \mathbf{R}$, where ∞ is allowed both as a limit value and as an element of the sequence $\{\phi_n(\mu)\}$. Define rate function $I(x) \triangleq \sup_\mu[\mu x - \phi(\mu)]$ and the set $D_I \triangleq \{x: I(x) < \infty\}$. Let $a, b \in$ IR. If $[a, b] \cap D_I \neq \varnothing$**, then**

$$\overline{\lim_{n\to\infty}} \frac{1}{n}\log P\{\tfrac{Y_n}{n} \in [a,b]\} \leq - \inf_{x\in[a,b]} I(x).$$

A. Application to integrate-and-dump receiver with ISI

The integrate-and-dump receiver's output $y\lambda$ can be viewed as an infinite sequence of random variables indexed by an increasing sequence of λ's. Consequently, the logarithm of each of the conditional MGFs, $\phi_\lambda(\mu|b_0)$ and $\phi_\lambda(\mu|b_1)$ in (17), is identified exactly with the quantity $\phi_n(\mu)$ in GartnerEllis Theorem. Next, we define $\phi_0(\mu) \triangleq \lim_{\lambda\to\infty} \phi_\lambda(\mu|b_0 = 0)$ corresponding to the case of $b_0 = 0$. By substituting (16) for $R_i(\mu)$ in (18b), we obtain

$$\phi_0(\mu) = \frac{1}{\lambda}\log\left[\prod_{k=1}^{\infty}\left(\frac{1}{2} + \frac{1}{2}\exp\left(\lambda\left[\frac{1}{T_b}\int_0^{T_b} A_k(\mu|\xi)d\xi - 1\right]\right)\right)\right]$$

$$= \sum_k\left(\frac{1}{\lambda}\log\left[\frac{1}{2} + \frac{1}{2}\exp\lambda\left[\frac{1}{T_b}\int_0^{T_b} A_k(\mu|\xi)d\xi - 1\right]\right]\right). \tag{20}$$

By the fact that

$$\lim_{\lambda\to\infty}\frac{1}{\lambda}\log\left[\frac{1}{2} + \frac{1}{2}\exp\left(\lambda x\right)\right] = (x)^+, \tag{21}$$

where $(\cdot)^+$ is a function defined as $(x)^+ = x$ for $x > 0$ and 0 elsewhere, we obtain

$$\phi_0(\mu) = \sum_k\left(\frac{1}{T_b}\int_0^{T_b} A_k(\mu|\xi)\,d\xi - 1\right)^+. \tag{22}$$

Similarly, we define $\phi_1(\mu) = \lim_{\lambda\to\infty}\phi_\lambda(\mu|b_0 = 1)$, corresponding to the case of $b_0 = 1$. Upon using (18a) and some analysis, we obtain

$$\phi_1(\mu) = \left(\frac{1}{T_b}\int_0^{T_b} A_0(\mu|\xi)d\xi - 1\right) + \sum_k\left(\frac{1}{T_b}\int_0^{T_b} A_k(\mu|\xi)d\xi - 1\right)^+. \tag{23}$$

The rate functions $I_0(x)$ and $I_1(x)$ can now be calculated from $\phi_0(\mu)$ and $\phi_1(\mu)$ by

$$I_i(x) = \sup_{\mu}[\mu x - \phi_i(\mu)], i = 0,1. \tag{24}$$

Let $\mu_0 \triangleq \inf_{x\geq\gamma} I_0(x)$ and $\mu_1 \triangleq \inf_{x\leq\gamma} I_1(x)$, where γ is the normalized threshold value (defined in (11)). Then, the application of the Gärtner-Ellis Theorem gives the following error bounds

$$\begin{aligned} P\{y_\lambda \geq \gamma_\lambda|b_0 = 0\} &\leq e^{-\lambda\mu_0}, \\ P\{y_\lambda < \gamma_\lambda|b_0 = 1\} &\leq e^{-\lambda\mu_1}, \end{aligned} \tag{25)(26}$$

and the BER can be upper bounded as

$$P_b \leq \frac{1}{2}(e^{-\lambda\mu_0} + e^{-\lambda\mu_1}). \tag{27}$$

SECTION V. Numerical Results

As the example presented in Section III, we consider a thin InP-based APD with a 100 nm multiplication layer. The APD is appropriated biased to yield an average gain of 10.65. The joint pdf of the gain and buildup time was numerically calculated using the renewal theory [19]. We consider the receiver operating at 40 Gbps and 60 Gbps transmission rates; the former rate is the speed corresponding to the OC-768 standard, which is the fastest synchronous optical network (SONET) standard, and the latter rate is chosen to further demonstrate the degrading effects of ISI. As before, we choose $m = 2$. Equations (22) and (23) are calculated numerically and the rate functions are also calculated numerically using (24). The normalized threshold γ is calculated by use of (11) yielding $\gamma \approx 5.32$. The decaying tails of the error probabilities are bounded by (25) and (26), with the numerically calculated $\mu 0 = \inf_{x \geq \gamma} I_0(x)$ and $u_1 = \inf_{x \leq \gamma} I_1(x)$. Finally, the BER is estimated using (27).

For different large values of λ, we calculated the BER estimate using (a) the LDT approach and (b) the exact MGF inversion approach. The behavior of the BER, as the average number of photons per bit, is shown in Figs. 4(a) and 4(b) for the two cases of transmission rate of 40 Gbps and 60 Gbps, respectively. These figures also include the results obtained using the Gaussian approximation method. In the latter method we assume that $Y\lambda$ follows a Gaussian distribution with a conditional mean and variance (depending upon whether $b_0 = 0$ or $b_0 = 1$); these statistics are easily computed from the pdf of r_k. As expected, the MGF inversion method yields the smallest BER; it also expected to offer the tightest estimate due to the fact that it utilizes the exact conditional pdfs of $y\lambda$. The LDT approach gives an upper bound of BER. Note that this bound has the same decaying rate as that given by the exact MGF inversion approach. In addition, this BER bound is significantly tighter than the one obtained by the Gaussian approximation method.
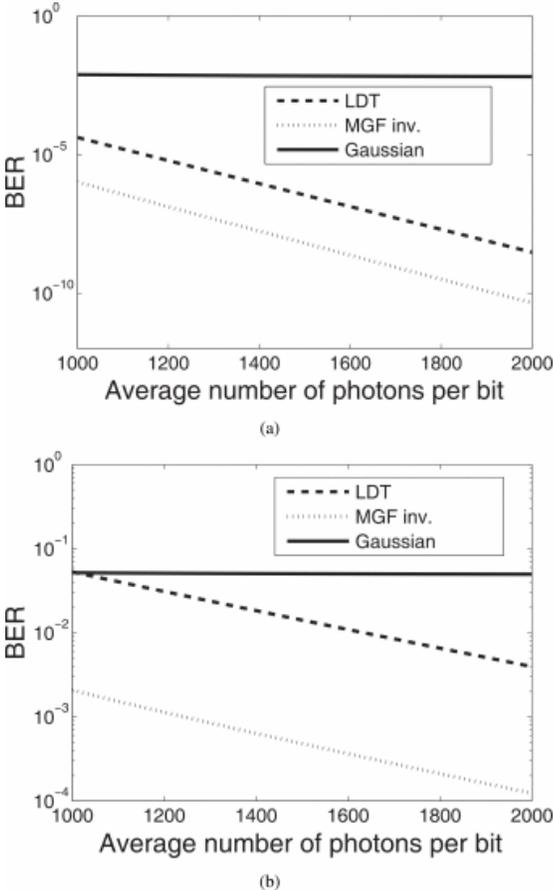
Fig. 4: Bit error rate as a function of average number of photons per bit for (a) 40 Gbps transmission and (b) 60 Gbps transmission.

The numerical results suggest that in the ultra-fast transmission scenarios considered, the Gaussian method is not appropriate. This is due to two primary factors: (a) the pdf of the subcomponent r_k has asymmetric shape and (b) the pdf of receiver output $Y\lambda$ has a bi-modal distribution. At lower transmission rates such as 10 Gbps, where ISI is almost negligible, the use of a unimodal distribution, such as the Gaussian distribution, may yield a approximation of the BER. For example, our calculations yield an error in the BER of 8.7×10^{-8} between the Gaussian approximation and the exact MGF method when the average number of photons is 1000 per bit and a BER error of 3.7×10^{-12} for the case of 1500 photons per bit. One possible approach for doing away with the uni-modal condition imposed by the standard Gaussian-approximation method employed in this paper is to employ the following simple variant of it. Instead of assuming a Gaussian pdf for the receiver output conditional on the present bit, we assume a Gaussian pdf for the receiver output conditional on the present bit *and* all the past bits. In this fashion, the pdf of the receiver output conditional on the present bit is allowed to be multi-modal, as it is the average of multiple heterogeneous conditional *bit-pattern–dependent* pdfs. However, the aforementioned alternative Gaussian-approximation method does come at a higher computational complexity compared to the standard Gaussian-approximation method.

We end this section by making the general comment that the performance of APD-based receivers deteriorates quickly as a function of the transmission speed due to ISI. This is evident from the poor BERs shown in Fig. 4(b) for transmission speeds of 60 Gbps. This limitation is primarily due to the avalanche buildup time, which reduces the operable bandwidth and induces ISI. One possible approach to extend the operability of APDs to high transmission speeds involves the use of electronic equalizers, as proposed by Sun and Hayat [30]; however, much work is needed to implement this approach.

SECTION VI. Conclusion

This paper provides a rigorous characterization of the BER associated the general class of APD-based optical receivers used in ultra-fast direct-detection communication. The analysis takes into account ISI resulting from the non-instantaneous nature of the APD's stochastic impulse response function, which is attributable to the so-called avalanche-buildup time, as well as the dead-space effect that is inherent in APDs with thin multiplication regions used in ultra-fast receivers. We have developed an exact expression for the MGF of the receiver's output using the joint pdf of the APD's gain and avalanche-buildup time. The MGF of receiver's output is then utilized to (a) calculate the BER exactly and (b) perform an asymptotic analysis of the BER yielding an upper bound for the BER based on the Gärtner-Ellis Theorem from large deviation theory. The results show that the Gaussian-approximation method is not suitable for ultra-fast transmission scenarios due to the presence of ISI, which tends to cause asymmetry and bi-modality in the shape of the probability density function of the receiver's output. Notably, the large-deviation based asymptotic analysis yields a much improved approximation of the BER compared to the Gaussian approximation and also offers the correct decay rate in the BER as a function of the average photons per bit.

References

1. G. Agrawal, Fiber-Optic Communication System, New York:Wiley, 2002.
2. B. E. A. Saleh, M. C. Teich, Fundamentals of Photonics, New York:Wiley, 2007.
3. K. Anselm, H. Nie, C. Hu, C. Lenox, P. Yuan, G. Kinsey, J. Campbell, B. Streetman, "Performance of thin separate absorption charge and multiplication avalanche photodiodes", *IEEE J. Quantum Electron.*, vol. 34, pp. 482-490, Mar. 1988.
4. K. F. Li, D. S. Ong, J. P. R. David, G. J. Rees, R. C. Tozer, P. N. Robson, R. Grey, "Avalanche multiplication noise characteristics in thin GaAs p+—i—n+ diodes", *IEEE Trans. Electron Devices*, vol. 45, pp. 2102-2107, Oct. 1998.

5. D. S. Ong, K. F. Li, G. J. Rees, G. M. Dunn, J. P. R. David, P. N. Robson, "A Monte Carlo investigation of multiplication noise in thin p+—i—n+ GaAs avalanche photodiodes", *IEEE Trans. Electron Devices*, vol. 45, pp. 1804-1810, Aug. 1998.

6. K. F. Li, D. S. Ong, J. P. R. David, P. N. Robson, R. C. Tozer, G. J. Rees, R. Grey, "Low excess noise characteristics in thin avalanche region GaAs diodes", *Electron. Lett.*, vol. 34, pp. 125-126, 1998.

7. C. Hu, K. A. Anselm, B. G. Streetman, J. C. Campbell, "Noise characteristics of thin multiplication region GaAs avalanche photodiodes", *Appl. Phys. Lett.*, vol. 69, pp. 3734-3736, 1996.

8. C. Lenox, P. Yuan, H. Nie, O. Baklenov, C. Hansing, J. C. Campbell, J. A. L. Holmes, B. G. Streetman, "Thin multiplication region inalas homojunction avalanche photodiodes", *Appl. Phys. Lett.*, vol. 73, pp. 783-784, 1998.

9. M. M. Hayat, O. Kwon, Y. Pan, P. Sotirelis, J. C. Campbell, B. E. A. Saleh, M. C. Teich, "Gain-bandwidth characteristics of thin avalanche photodiodes", *IEEE Trans. Electron Devices*, vol. 49, pp. 770-781, May 2002.

10. S. Wang, R. Sidhu, X. G. Zheng, X. Li, X. Sun, J. A. L. Homes, J. C. Campbell, "Low-noise avalanche photodiodes with graded impact-ionization-engineered multiplication region", *IEEE Photon. Technol. Lett.*, vol. 13, pp. 1346-1348, Dec. 2001.

11. P. Yuan, S. Wang, X. Sun, X. G. Zheng, J. A. L. Holmes, J. C. Campbell, "Avalanche photodiodes with an impact-ionization-engineered multiplication region", *IEEE Photon. Technol. Lett.*, vol. 12, pp. 1370-1372, Oct. 2000.

12. M. Achouche, V. Magnin, J. Harari, F. Lelarge, E. Derouin, C. Jany, D. Carpentier, F. Blache, D. Decoster, "High performance evanescent edge coupled waveguide unitraveling-carrier photodiodes for > 40-Gb/s optical receivers", *IEEE Photon. Technol. Lett.*, vol. 16, pp. 584-586, Feb. 2004.

13. M. A. Saleh, M. M. Hayat, B. E. A. Saleh, M. C. Teich, "Dead-space-based theory correctly predicts excess noise factor for thin GaAs and AlGaAs avalanche photodiodes", *IEEE Trans. Electron Devices*, vol. 47, pp. 625-633, Mar. 2000.

14. X. Li, X. Zheng, S. Wang, F. Ma, J. C. Campbell, "Calculation of gain and noise with dead space for GaAs and AlxGa1—xAs avalanche photodiode", *IEEE Trans. Electron Devices*, vol. 49, pp. 1112-1117, July 2002.

15. R. J. McIntyre, "Multiplication noise in uniform avalanche photodiodes", *IEEE Trans. Electron Devices*, vol. ED-13, pp. 164-168, Jan. 1966.

16. M. M. Hayat, B. E. A. Saleh, "Statistical properties of the impulse response function of double-carrier multiplication avalanche photodiodes including the effect of dead space", *IEEE J. Lightwave Technol.*, vol. 10, pp. 1415-1425, Oct. 1992.

17. X. Li, X. Zheng, S. Wang, F. Ma, J. C. Campbell, "Calculation of gain and noise with dead space for GaAs and AlxGa1—xAs avalanche photodiode", *IEEE Trans. Electron Devices*, vol. 49, pp. 1112-1117, July 2002.

18. M. M. Hayat, G. Dong, "A new approach for computing the bandwidth statistics of avalanche photodiodes", *IEEE Trans. Electron Devices*, vol. 47, pp. 1273-1279, 2000.

19. P. Sun, M. M. Hayat, B. E. A. Saleh, M. C. Teich, "Statistical correlation of gain and buildup time in APDS and its effects on receiver performance", *IEEE J. Lightwave Technol.*, vol. 24, pp. 755-768, 2006.

20. S. D. Personick, "Statistics of a general class of avalanche detectors with application to optical communication", *Bell Syst. Tech. J.*, vol. 50, pp. 3075-3395, 1971.

21. M. M. Hayat, B. E. A. Saleh, J. A. Gubner, "Bit-error rates for optical receivers using avalanche photodiodes with dead space", *IEEE Trans. Commun.*, vol. 43, pp. 99-107, Jan. 1995.

22. S. D. Personick, P. Balaban, J. H. Bobsin, "A detailed comparison of four approaches to the calculation of the sensitivity of optical fiber system receivers", *IEEE Trans. Commun.*, vol. 25, pp. 541-548, 1977.

23. C. Helstrom, "Performance analysis of optical receivers by the saddlepoint approximation", *IEEE Trans. Commun.*, vol. 27, pp. 186-191, 1979.

24. K. B. Letaief, J. S. Sadowsky, "Computing bit-error probabilities for avalanche photodiode receivers by large deviations theory", *IEEE Trans. Inform. Theory*, vol. 38, pp. 1162-1169, 1992.

25. J. S. Sadowsky, J. A. Bucklew, "Large deviation theory techniques in monte-carlo simulation", *Proc. 1989 Winter Simulation Conf.*, pp. 505-513, 1989.

26. B. Choi, M. M. Hayat, "Computation of bit-error probabilities for optical receivers using thin avalanche photodiodes", *IEEE Commun. Lett.*, vol. 10, pp. 56-58, Jan. 2006.

27. C. Groves, J. David, "Effects of ionization velocity and dead space on avalanche photodiode bit error rate", *IEEE Trans. Commun.*, vol. 55, pp. 2152-2158, Oct. 2007.

28. J. A. Bucklew, Large Deviation Techniques in Decision Simulation and Estimation, John Wiley and Sons, 1990.

29. R. S. Ellis, "Large deviations for a general class of random vectors", *Ann. Probability*, vol. 12, no. 1, pp. 1-12, 1984.

30. P. Sun, M. M. Hayat, "A linear equalizer for high-speed APD-based integrate-and-dump receivers", *IEEE Commun. Lett.*, vol. 9, pp. 1073-1075, 2005.

Keywords

IEEE Keywords

Bit error rate,

Optical receivers,

Intersymbol interference,

Optical noise,

Electron optics,

High speed optical techniques,

Ultrafast optics,

Sun,

Stochastic processes,

Avalanche photodiodes

INSPEC: Controlled Indexing

avalanche photodiodes,

error statistics,

intersymbol interference,

optical communication,

optical receivers,

photodetectors

INSPEC: Non-Controlled Indexing

bit error rate,

ultrafast APD,

optical receiver,

exact analysis,

asymptotic analysis,

large-deviation theory,

ultrafast avalanche-photodiode,

intersymbol interference,

stochastic avalanche buildup time,

transmission rate,

bit duration,

BER analysis,

ISI noise,

optical communication

Author Keywords

Optical communication, avalanche photodiodes, optical receivers, optoelectronic devices, error analysis, large deviation principle.